6. Till Deformation with Clasts: laboratory experiments

6.1 Introduction

6.1.1 Overview

When the first models of the basal movement of glaciers were being devised it was realised that the problem with modelling motion over a hard bed was not how movement could develop, for ice should move unrealistically fast on a smooth bed. Rather the problem was how to model reasonable, slower, glacier speeds while still allowing any movement at all (Weertman, 1957). A similar problem has been posed with regards more recent soft bed models. Movement over a *deforming* bed of till may give high glacier velocities (Boulton *et al*., 1974; Boulton and Jones, 1979). However, Kamb (1991) has shown that the vital problem with the soft bed model is, again, that the velocities produced may be far *too* high to be realistic.

Subglacial till deformation has been modelled as a viscose material (Boulton and Hindmarsh, 1987; Clarke 1987; Alley 1991)

$$\dot{e} = a t^{n} P_e^{m} \qquad \text{...Equation 6.1}$$

where t is the effective basal shear stress, P_e is the basal effective normal stress, $\dot{e}$ is the strain rate, and a, n, and m are empirically derived constants. The potential for non-linear behaviour is given by n and m.

Fitting this model to field data, Boulton and Hindmarsh (1987) suggest n ≈ 1. Clarke (1987) also uses a linear stress response. Kamb (1991), however, suggests n ≈ 100 on the basis of laboratory experiments.

6.1.2 Kamb's shear box analogue

Kamb (1991) ran shear box tests (Bolton, 1979) (*Figure 6.1*) on sediment from the base of Ice Stream B in Antarctica. Clasts ≥ 10 mm were removed from the sample. Under constant stress tests a threshold stress was identified between low stress work-hardening and high stress catastrophic work-softening. All movement occurred across a thin shear zone. The

terms work-hardening and work-softening are used here to indicate a lowering or raising of the shear rate with strain at a constant shear stress. They are also used to indicate an increase or decrease of the supported stress with strain at a constant shear strain rate. The ideal terms for this behaviour 'strain hardening and strain softening' are already in use to describe changes in behaviour with initial shear strain rate.

Using constant strain rate tests the stress threshold was found to match the residual strength of the material. The sediment showed a typical silt strain response, undergoing work-hardening at a decelerating rate until a constant 'residual' stress was supported (for example, *Figure 3.7*). There was no peak supported stress which could be identified as a failure or 'yield' point, therefore 'residual stress' is used in preference to Kamb's 'yield strength'. A coincidence of residual and yield strengths is not unusual for reformed sediments. Kamb's conclusions for glacial dynamics are intimately connected with his nomenclature.

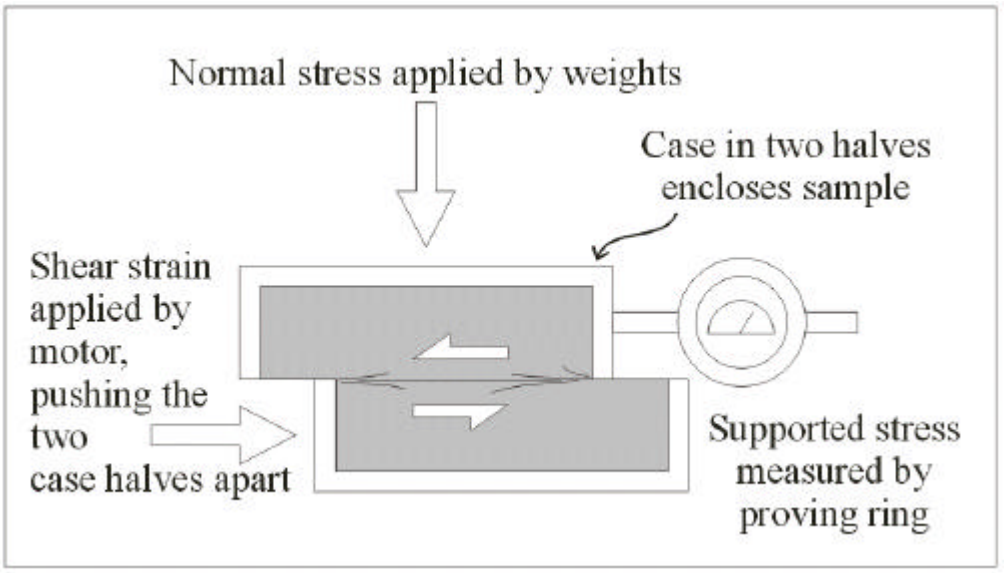

Figure 6.1 The simple shear box method. Sample shears at a point between the two halves of the containing box, forced by the box geometry.

Kamb described the catastrophic work-softening of the material as a highly non-linear response to shear stress, so non-linear in fact, that it could be considered as instantaneous and modelled by $n \approx 100$ in Equation 6.1. This is a reasonable, though unrepresentative, model of this behaviour. The non-linear viscose model describes a change in strain rate with stress. Kamb found a change in the strain rate as strain progressed, but with a stress threshold. This substitution is reasonable as long as the rate of work-hardening/softening is rapid. Given such non-linear behaviour, Kamb proposed that there could be no bed friction under a soft-bedded glacier with a basal shear stress greater than the threshold value. This includes most glaciers, therefore, another mechanism must be controlling glacial velocities (Boulton and Jones, 1979, use a similar model, but with a higher threshold).

However, a corollary of this model is the glacial shear-stress would be wholly released across a thin shear zone. Thus, there could be no transferral of stress deeper into the sediment (contrast with field work in Boulton and Hindmarsh, 1987), and no vertically extending deformation structures in palaeo-tills, only meltout features from deformed debris-rich ice (contrast with Paul and Eyles, 1990). The model is therefore incomplete. The catastrophic failure of the sediment in Kamb's experiments is probably a consequence of the experimental technique. The simple-shear 'shear box' set-up used constrains the development of shear planes. These propagate from the interface between the two box halves rather than spreading through the sediment. In natural simple shear, shears form at an angle to the horizontal, interact, and then develop into a Principle Displacement Zone with a complex internal geometry (Chapter Three). In nature there will also be a complex interaction between the shear strain and hydrological response which is not accounted for in such undrained shear tests.

These shear development problems are exacerbated by the removal of clasts larger than 10 mm from the samples. With a shear box height of 25 mm, it is quite possible that the shears never included clasts in their plane, or that any clasts were expelled from the shears until they did not straddle the interface between the two boxes. If shears pervaded the sample they would be forced to interact with clasts as the density of both shears and clasts increased.

The 'triaxial rig' set-up (*Figure 6.2*) can counter the problems of grain size distribution to a greater extent, and allows free development of shear zones. However, the equipment is limited to strains below ~ 30%; the progression to infinite strain cannot be studied. 'Ring-shear' rigs, can produce infinite strains but have not yet been used to provide hydrologic information with sediments of a size range suitable for glaciology. Iverson *et al*. (1996) tested suitable material, and Brown *et al*. (in press) included hydrodynamics, but no one has tested both. Ring shear rigs also force shear zone geometries. Thus, a series of triaxial tests were run on material sampled from the Skipsea Till at Skipsea in Yorkshire (*Figure 6.3*). The next section outlines the reasoning behind the methods employed and the limitations on the specific situations that can be recreated. The section following this outlines the details of these methods and the test conditions used.

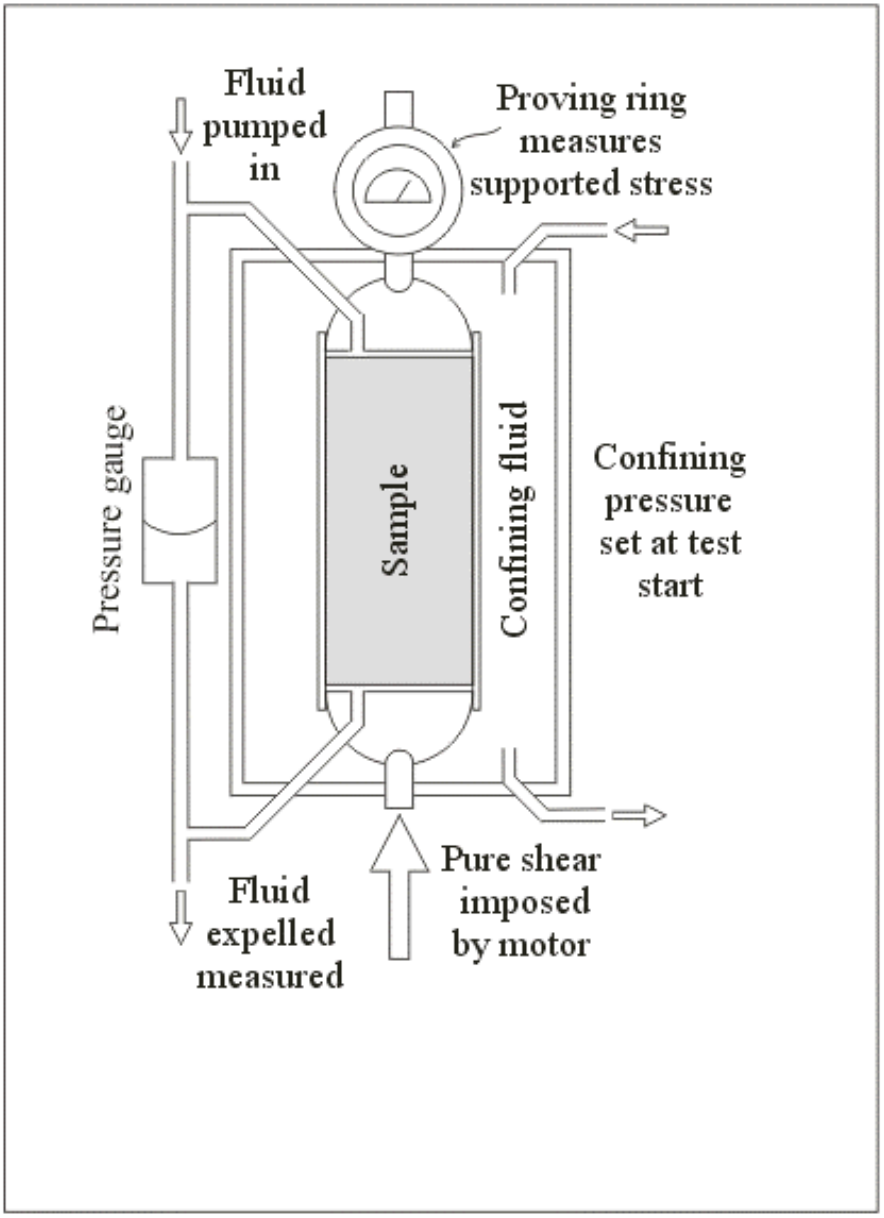

Figure 6.2 The triaxial deformation apparatus used in the experiments.

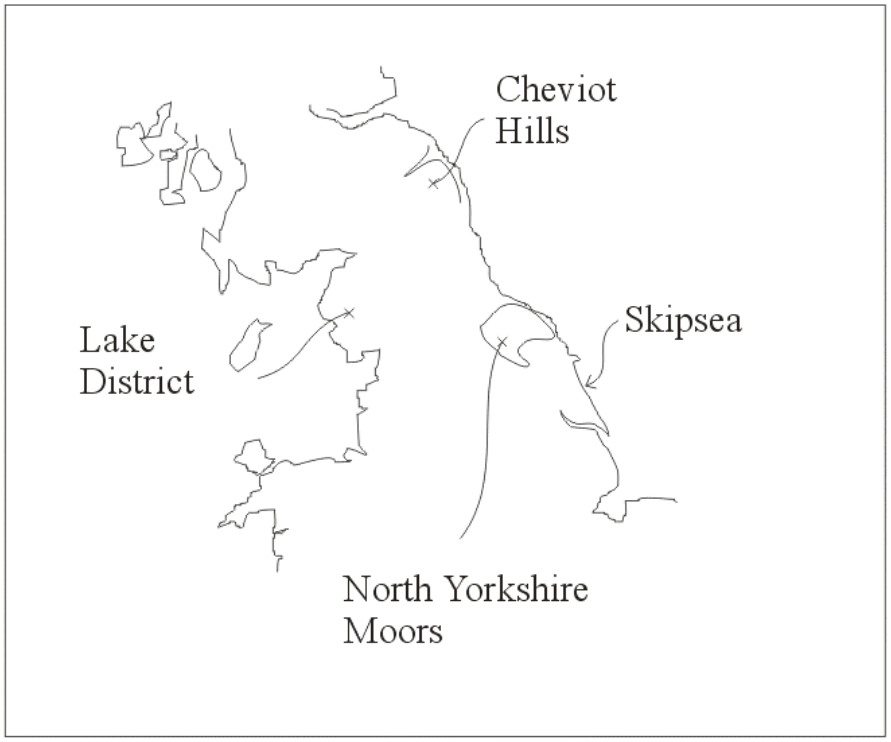

Figure 6.3 Location of sample site and sites discussed in the text.

6.2 Methods

6.2.1 Creating an analogue for subglacial deformation

It is an over-simplification to model subglacial deformation on the basis of one experimental set-up. Deformation is likely to be heterogeneous and dependant on the ice history, the ice-sediment interface, and the clast density in the sediment and basal ice. As well as steady state deformation, the deformation boundary may rise and fall during the glaciation (Hart *et al.*, 1990). The ice-sediment interface may be smooth (Clarke, 1987), the ice may move into the sediment (Boulton and Hindmarsh, 1987; Iverson and Semmens, 1995), or the stress may be transferred by an irregular ice base topography or clasts (implicit in Alley, 1989; also Chapter Five).

Clasts may bridge the deformation front or ice interface, and the stress conditions they impose will be dependant on their density and the sediment response. For example, a pure strain geometry will exist between two clasts trapped at different heights in a deforming layer where the velocity drops with depth (*Figure 7.3*). Where clast density is lower, there may be no

depth overlap between clasts and it may be possible to approximate the sediment deformation as simple shear.

The response of deforming sediments is extremely sensitive to the imposed stress magnitude and direction. It is therefore essential in tests that the stress conditions, including the hydrological changes, are as close as possible to those found subglacially. It is also important to specify which subglacial situations are being recreated. Each set of equipment is an analogue for only certain situations (*Figure 6.4*). A general model of deformation will only be successful when the rheological response of several bed situations can be combined. Triaxial tests recreate two important situations.

1) The initial ploughing of boulders or irregular basal ice into undeformed sediment. Such sediment could be under a descending deformation front.
2) The deformation of sediment trapped between clasts. A clast trapped in the ice, or in higher strain rate sediment, will transfer stress through the sediment to downstream clasts on the same horizontal. If Kamb's shear-box experiments show the response of matrix without clasts, clast interactions may be the most important mechanism for the transfer of stress into soft-beds. The time over which the clasts interact will determine the period over which stress is transferred deeper into the sediment. Clast-clast interactions will also take place *within* triaxial samples.

The flow of material around clasts is a crucial addition to the stress transfer, thus it is unnecessary to run the tests under the zero lateral strain (sometimes known as K_0) conditions commonly sought for in other environmental reconstructions.

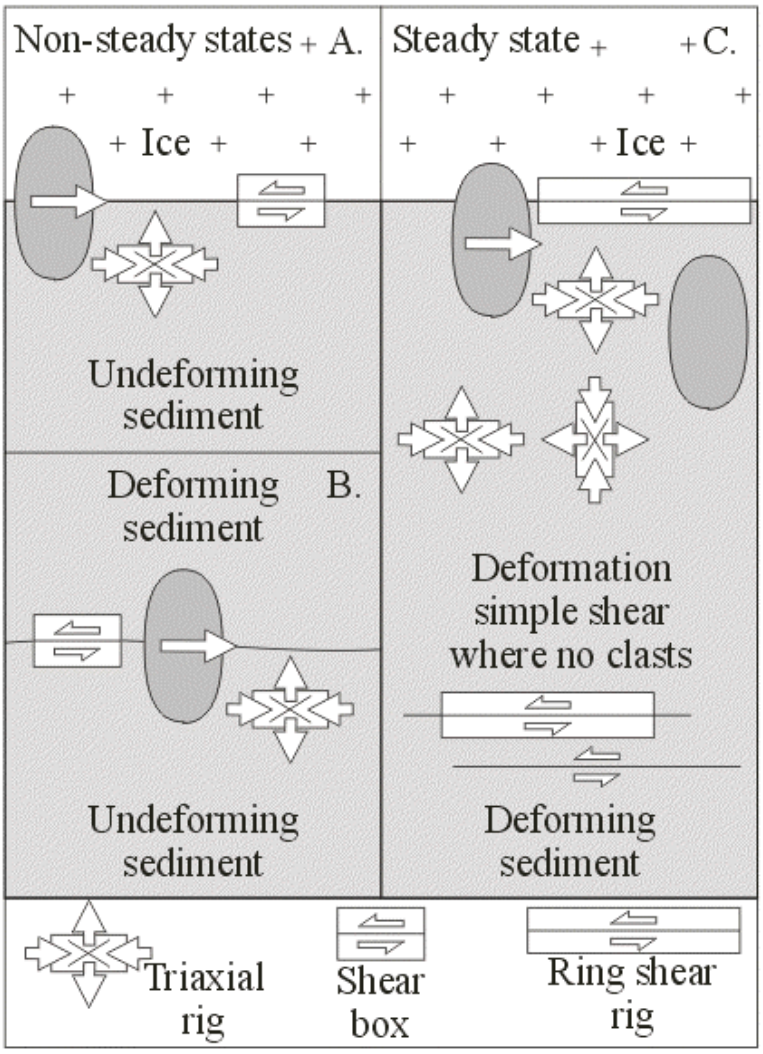

Figure 6.4 Subglacial situations for which different deformational equipment is analogous. A. Clast trapped in a smooth ice base ploughs through undeformed sediment. Conditions similar to those in a triaxial rig exist in front of the clast (arrows show force directions). Conditions similar to a shear box exist at the smooth ice-bed interface. B. Clast trapped in fast moving till ploughing through undeforming sediment. Conditions similar to those in a shear box exist at décollements within the sediment. C. In steady state deformation conditions similar to triaxial and shear box experiments exist, as well as conditions similar to ring shear rigs.

The subglacial conditions that must be recreated are;

1) applied confining stresses ranging between ~10's m to 2000 m of ice.
2) pore fluid pressures ranging from zero to above the confining stress.
3) rates of water inflow (for warm bedded glaciers) such that a pore-fluid head will build-up if the sediment remains homogeneous (Boulton and Hindmarsh, 1987).
4) rates of compression in front of solid clasts locked in the ice from 0.00379 mm min^{-1} (2 m a^{-1}) to 3.79 mm min^{-1} (2000 m a^{-1}).

The most difficult condition to reproduce is the excess fluid inflow. The fluid influx from warm bedded glaciers rises above the discharge capacity of subglacial sediments both seasonally and diurnally. Seasonal variations are concentrated in areas that eventually pipe and become channelled as the meltwater flux increases (Boulton and Hindmarsh, 1987; Walder and Fowler, 1994). For a typical Alpine glacier and a range of likely sediments, the distance affected by high rainfall events around the channel may be between 5 and 80 m (Hubbard et al., 1995; A.Barrett and D.Collins, pers.comm., 1996). The rheology and size of the areas which do not pipe will be controlled by the drainage response of the sediment as the effective pressure moves towards zero. The drainage capacity is controlled by structures formed during deformation (Chapter Three).

Triaxial tests are usually run so that the sediments are either undrained (rapid tests) or fully drained (pore-pressures allowed to adjust by straining slowly compared to the drainage). These tests correspond to engineering situations relevant to the stability of constructions. The response of sediments to non-equilibrium conditions are rarely examined. The inflow in tests must be constrained such that leakage does not occur between the sleeve and the sample. In an effort to reproduce glacial levels of strain and inflow these restrictions were ignored. Fluid pressures were allowed to build up under the assumption that the record up to the point of sleeve leakage would more accurately reflect the natural development of the sediments. As it happens, internal changes in the sediment decrease the excess pressure prior to the leak point. The pore fluid pressure could have been raised manually during the tests, however, this would have obscured a number of interesting processes, for example, the relationship between yield fabric development and the fluid pressure.

6.2.2 Samples and equipment set-up

A till block was removed from the Skipsea till exposed at Skipsea on the Yorkshire coast (*Figure 6.5*). The sample was taken from a homogeneous cliff of diamict with no low strain features in it (including dilation or shear horizons such as described by Boulton and Hindmarsh, 1987). The area sampled was 500 m south of a set of canal deposits (D.Evans, *pers.comm.*, 1996, see also Walder and Fowler, 1994).

Approximately 1 km south of this position lie the Skipsea Mere deposits. These deposits are the remains of a lake system drained in medieval times that lies on the sub-Devensian topography of Anglian tunnel valleys (Sheppard, 1957). These tunnel valleys were undoubtedly low topographic points during subsequent glaciations and may well have been controlling the subglacial drainage layout. Thus, the sample area is in an area that may have experienced considerable subglacial fluid pressure fluctuations seasonally, and possibly diurnally, if the glacier was warm-bedded.

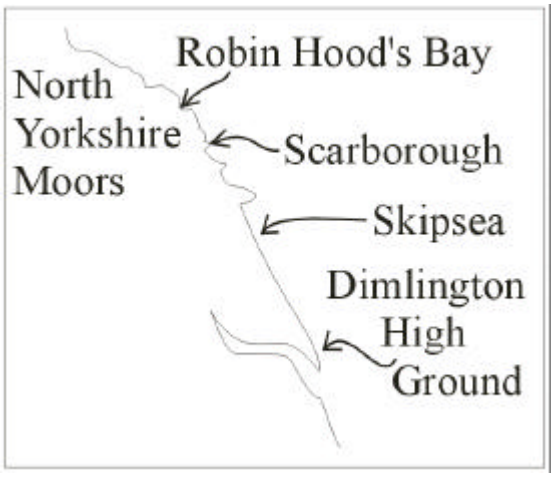

Figure 6.5 Locations around Skipsea

The block was removed 4 m below the cliff top after 1 m depth of till was removed from the cliff surface. The ambient stress conditions were not of interest, so the samples were allowed to dry under normal room temperature. Drying allowed cylinders of material to be cut from the block without disturbing their internal fabric. The block was cut into 50x50x120 mm sections with a wood saw, which were planed down to cylinders of 38 mm radius and 76 mm length using a knife. Clasts crossing the cylinder edges were trimmed flat to the sides with a hacksaw (if soft), or removed (if hard and could be removed without disturbing the surrounding material). Empty 'casts' were filled with a mix of wood glue and ground sample material as a hard, impermeable, and neutrally buoyant pebble replacement. If neither option was possible the sample was discarded. Samples frequently split along horizontal planes, suggesting a fabric in this direction. It was impossible to prepare cylinders with the original horizontal plane along the long axis of the cylinders, as the stress from the preparation techniques activated these weak planes. Typically samples took two days to prepare, with a failure to success ratio of 3.5:1. Table 6.1 summarises the mineralogy and grain size of the till.

Mean carbonate content (<2 mm fraction)	13.1%
Mean silt content	37.6% (32.8 to 42.4%)
Mean sand content	33.5% (22 to 45%)
Mean clay content	29% (21 to 37%)
Clay types	kaolinite, illite, vermiculite, smectite

Table 6.1 Mineralogy and grain size of the Skipsea Till (After Madgett and Catt, 1978; Goodyear, 1962) As will be shown in Chapter Seven, the size and mineral distribution of the material varies significantly on the scale of the triaxial samples.

Samples were tested in a triaxial rig in the Sediment Deformation Laboratory of the Institute of Earth Studies, University College of Wales, Aberystwyth. The triaxial rig (*Figure 6.2*) is of the standard type (for example, Vickers, 1983), with the exception of alterations to allow hydraulic measurements. The hydrology is determined by;

1) inflow into the top of the sample (computer controlled via an automated syringe);
2) outflow from the sample base (measured by a computer controlled piston);
3) the pressure at the sample base (controlled by the piston, which is set to maintain a constant 'back' pressure, while changing volume);
4) the fluid pressure across the sample (which is measured by a diaphragm pressure gauge connected in parallel with the sample).

Parameters measured in these tests were;

1) the supported stress at a constant strain rate;
2) the difference between the fluid pumped in for an interval and that exiting the sample, that is, the extra storage during any one interval;
3) the fluid pressure difference between the top and base of the sample, which gives the pore fluid pressure at the top of the sample (given the back-pressure).

Because the sediment response changes as its microscopic structure develops, thin sections were prepared from the samples after straining (examined in Chapter Seven).

Tests should be run with confining pressures greater than 600 kPa to prevent leakage between the sample and its rubber sleeve (which would render the tests 'fully drained'). The back pressure is usually run at half the confining pressure or less for the same reason. A number of tests (*Table 6.2*) were run prior to this becoming apparent and should, therefore, have a pore

fluid pressure constantly at the back pressure throughout the tests. This is not the case, so it seems that leakage was either partial or non-existent.

The strain rate was chosen such as to take around two days to reach ~25% strain. This rate was chosen on the basis of the equipment, constraints on lab time, the maximisation of any pre-leak record, and as falling near glacial velocities (equipment constraints limited the closest strain rates to ~3 m a^{-1} ice velocity). The inflows used ranged between 0.001 and 0.004 ml min^{-1} (464.71 mm a^{-1} to 2323.57 mm a^{-1} melt). This influx rate was the lowest possible when the tests began. The rate is a little high for basal melt rates (~100 mm a^{-1}), however, it falls between basal melt and flux through a small subglacial channel. The temperature of the apparatus used could not be lowered to subglacial levels, so the material was not tested in a frozen state.

Test	Confining pressure (kPa)	Starting back pressure (kPa)	Sample interval (s)	Fluid inflow (mm^3 m^{-1} / m a^{-1} melt)	Deformation rate (mm m^{-1} / m a^{-1})
D1	Equipment failed to record				
D2	500	300	174	1 / 0.52	$4.14x10^{-3}$ / 2.18
D3	500	325	144	4 / 2.08	$5.97x10^{-3}$ / 3.15
D4	Sleeve punctured at test start				
D5	660	330	87	2 / 1.04	$6.85x10^{-3}$ / 3.61
D6	660	330	44	1 / 0.52	$6.11x10^{-3}$ / 3.22

Table 6.2 Conditions of triaxial test runs.

Samples were pressurised to the confining pressure (though the material was too dry to respond) then fluid was pumped in at both ends to give an 'effective' confining pressure. Initial saturation of each sample took approximately two days. Saturation is determined to have occurred when the sample reaches a constant back pressure. Throughflow was then instigated and the material's pore space allowed to come into equilibrium with the throughflow and confining pressure. Equilibrium is marked by a halt in size change of the sample, measured by the difference between the fluid flowing in and that flowing out. Equilibrium took approximately six hours for these samples.

During saturation and equilibrium the sediment may be expected to have passed through the pressures between the initial confining pressure and the 'effective' confining pressure. The data presented by Boulton and Dobbie (1992; their figure 16-b) suggests the samples have previously been consolidated under pressures between 500 kPa and 600 kPa

(‘*preconsolidation pressures*’). These figures are gained (here) by assuming the site was subjected to an overburden between Boulton and Dobbie’s maximum at 1 m above sea level, (in a lower till unit at their location), and the overburden 4 m below the top of their Skipsea layer. The latter gives a minimum by assuming the top of the section at Skipsea was the top of the Skipsea till. Sediments undergoing *fully-drained* tests have a smaller porosity change with stress than expected up to their preconsolidation pressure. Given these values, it is more than likely that the Skipsea material will pass through its preconsolidation pressure while saturating, then become normally consolidated as the pore pressure reaches the backpressure. It is unknown what effects may be inherited from the overconsolidated state when the pore-fluid levels are altered in the sample.

6.3 Results

6.3.1 Stress response

Stress - strain diagrams are presented below for the four successful test runs in Figure 6.6. The initial strain at low stress values is an artefact of the equipment adjusting to the irregular surface of the samples. Unimodal, normally consolidated material usually responds to strain by reaching a level stress plateau after 5-7%. Features to note are;

1) the increase in stress supported with confining pressure (in line with *Equation 3.1*) - other factors also affect this relationship (see below), for example compare D2 and D3, both run at ~300 kPa effective confining pressure;
2) the large difference between D5 and D6, despite identical confining pressures.
3) supported stress drops in tests D2 and D3 at <2.5% strain;
4) supported stress drops in tests D2, D5 and D6, and a stress plateau followed by rise in D3 between 6 and 8%;
5) strain hardening (starting around 7%) intensifying in D3 (at 9.5%), D5 (at 11.5%) and D6 (at 14.5%). In samples D5 and D6 this supported stress profile is stepped, with periods of constant stress.

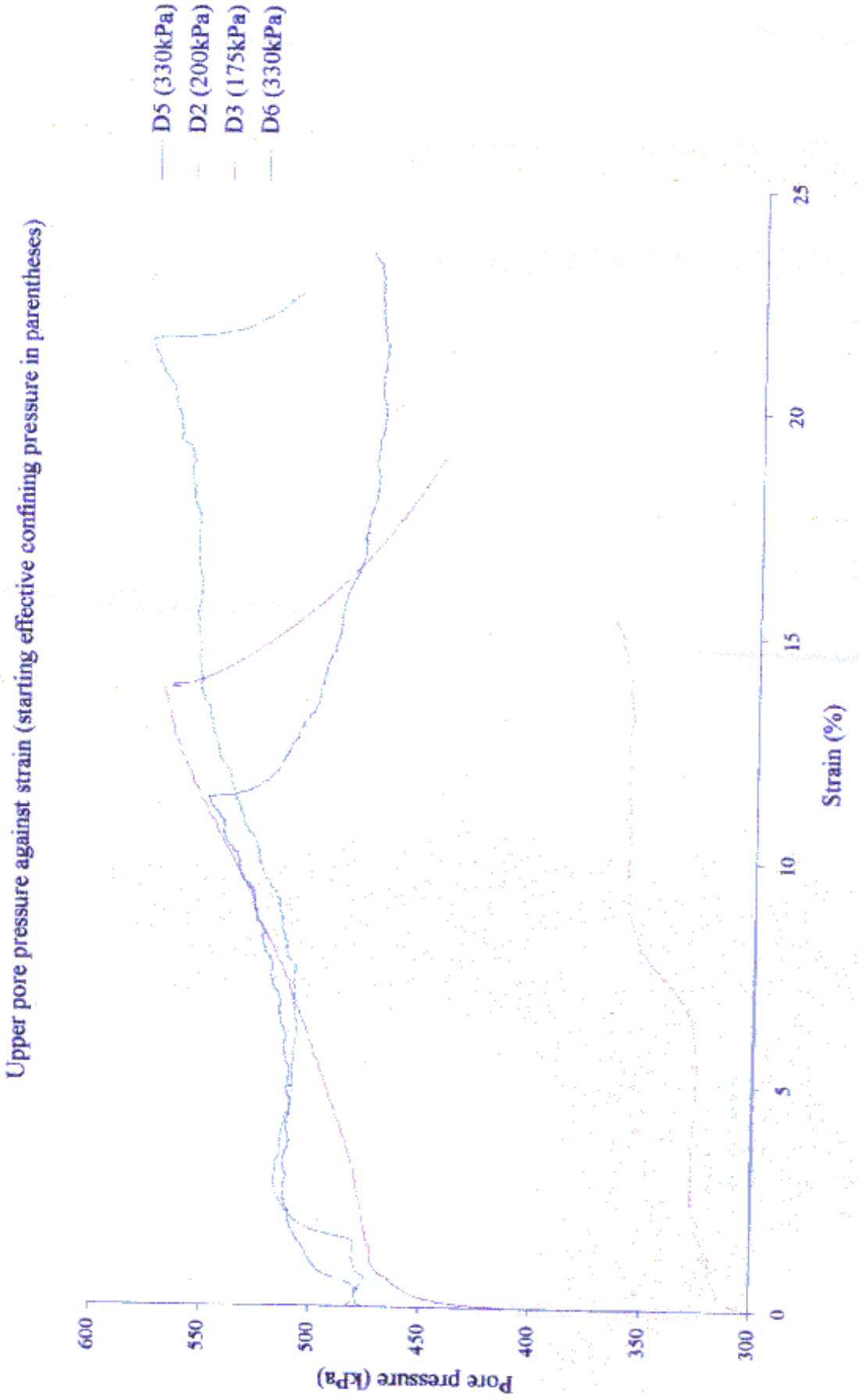

Figure 6.6 Stress-strain records for the triaxial tests.

6.3.2 Storage response

The storage response of the sediments is presented in Figure 6.7. The difference in signal variation for each test is considered to be a consequence of the change in equipment between tests D2 and D3, and D5 and D6. During these intervals the method of converting the signals from the fluid inflow and outflow pumps to signals suitable for recording on a computer was changed. The signal fluctuations are regular for tests D3 and D5 (wavelength of ~1% strain) between 12 and 15% strain. Test D3 has a response suggestive of at least two different wavelengths (~1% and ~12% strain). Both the short term regularity and longer term variation suggest the variations are instrument noise The change is probably due to a change in the signal processing between the input syringe and computer between the two tests. Thus, only the broad changes are regarded as experimentally useful and there is some suspicion that these mimic the temperature of the laboratory in D3, which may have varied during this particular test.

While none of the tests have an identical response, similarities exist.

1) In tests D2 and D5 the storage increased during the initial rise in stress up to 5 to 6.5% strain, then fell temporally to net expulsion as the stress dropped (at 6.5% for D2, and at 8 and 11.5% for D5). In both cases storage fell off at high strains.

2) Cumulative storages over the whole of the tests were (as percentages of the sample volumes) 0.616 % (D2), 0.278% (D5), 6.072% (D6), 20.477% (D3). The latter figure is far too large a porosity change. Given that most of the samples had a porosity (gained during the saturation of the sample from a air dried state) of ~40%, an extra 20% would leave cylinder D3 near its liquid limit at atmospheric pressure. However, at the end of test D3 the sample was still stiff enough to remove from the rig without deformation. This observation, in combination with the wave-like form of the storage response at least two scales, suggests the signal is a total artefact and is dismissed for D3. The signal for D6 appears more genuinely to vary with the other measured parameters, however, follows an opposite trend to D2/5 up to the end of the test, when a supported stress drop is matched by a drop in the net storage, possibly suggestive of expulsion.

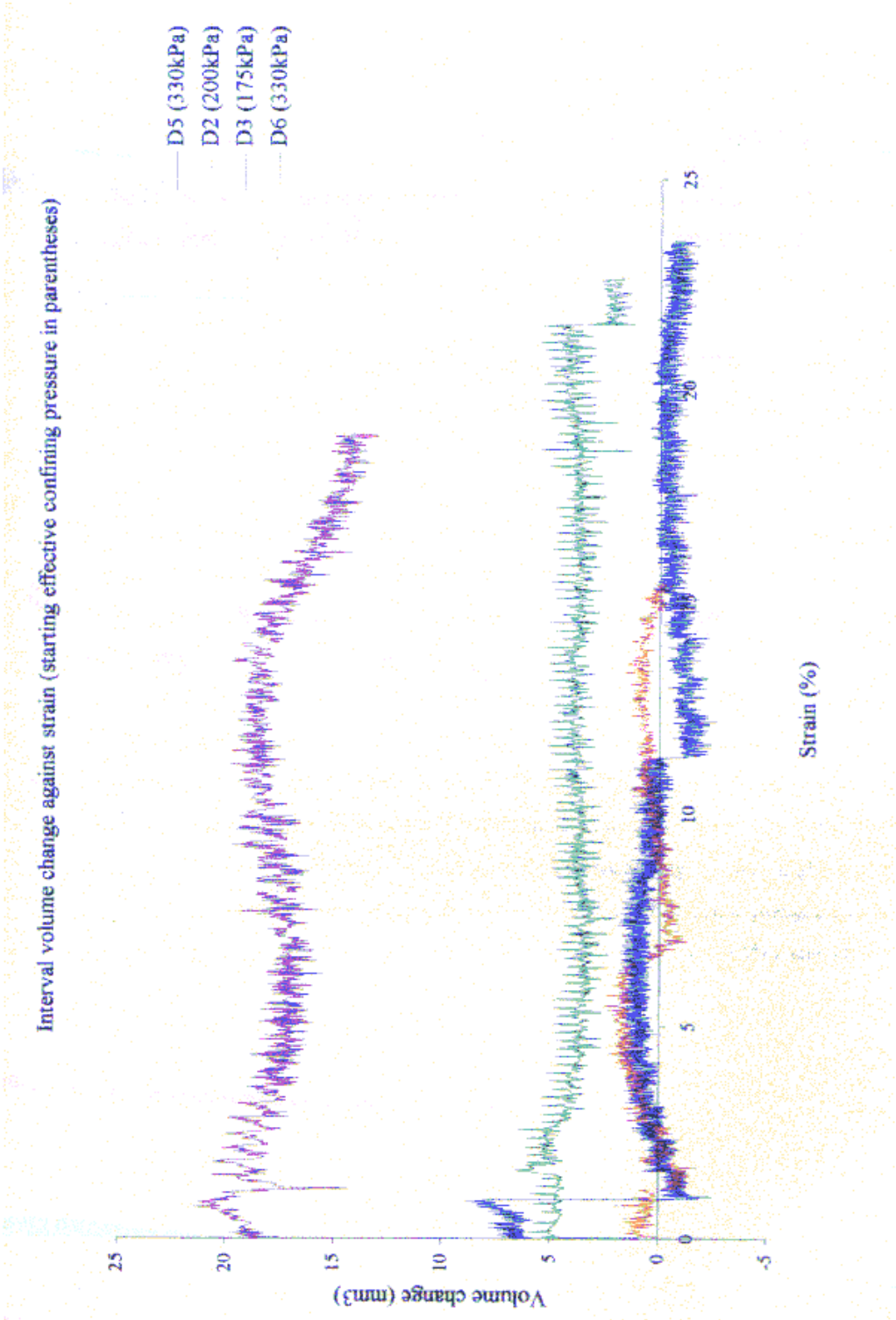

Figure 6.7 Storage records for the triaxial tests.

6.3.3 Upper pore pressure response

The upper fluid pore pressure (*Figure 6.8*) is allowed to equilibrate prior to the stress being applied, thus the initial ramping of pressure is not a machine artifice. There are a number of important features of the experimental records to note.

1) The initial rise in pressure of ~50 kPa in all the tests. These rises begin when stress starts to register for test D5 and D6, and slightly before for tests D2 and D3. As the conditions during adjustment to straining are unknown the latter results could still be due to stress application.
2) The steady *drop* of pressure (~10 kPa) to a new plateau (still higher than the start pressure) in tests D5 and D6. This is not matched in test D2, which simply reaches a plateau without falling. Test D3 never reaches a steady level, but does decline in slope.
3) The later ramping of pressure to a higher plateau (~50 kPa added) in samples D2 (at 7%) and D6 (at 8%). In both cases this is synchronous with a stress drop and fluid expulsion not seen in the two other samples. A lesser example of this behaviour is also seen at 2% strain in D2.
4) The rapid rise in pressure to a maximum for each sample followed by a rapid pressure drop to approximately the starting level. Each rise is synchronous with a stress drop or temporary plateau in stress, though in the case of D3 the drop is not that associated with the onset of work-hardening as in the other cases. The rapid fluid pressure drop would appear to accentuate the work-hardening, as one might expect from a greater effective confining pressure. However, fluid pressure changes cannot be responsible for the increase rate of hardening seen in D3 (at 9.5%) and D6 (at 14.5%).

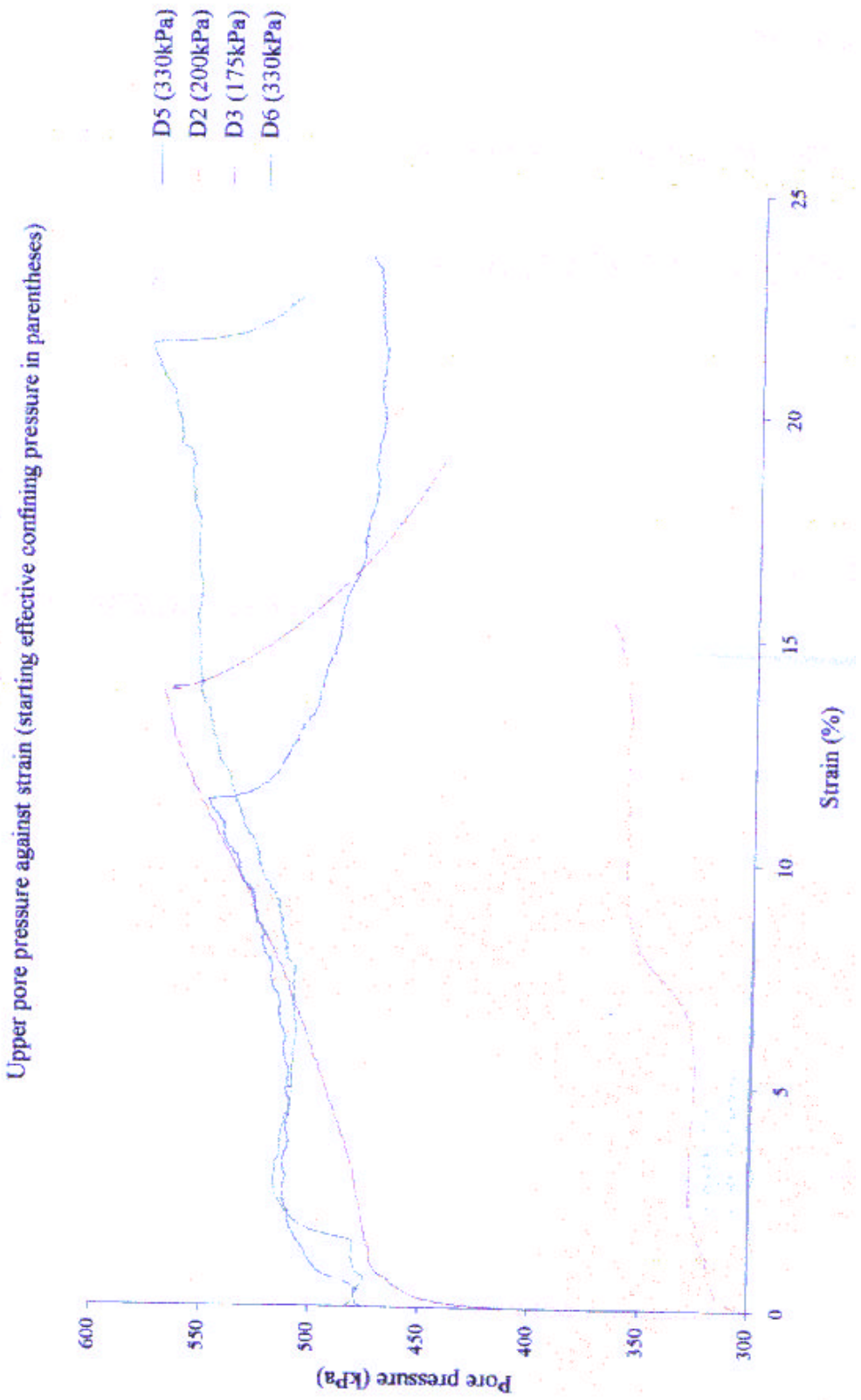

Figure 6.8 Upper pore fluid pressure record for the triaxial tests.

6.3.4 Stress paths

The average stress (p), average effective stress (p') and deviatoric stress (q) are defined (Jones, 1994) as

$$p = \frac{\left(s_a + 2s_c\right)}{3}$$

$$p' = \frac{\left(\left(s_a - P_p\right) + 2\left(s_c - P_p\right)\right)}{3}$$

$$q = \frac{\left(s_a - 2s_c\right)}{3}$$

where s_a is the supported stress measured on the proving ring and s_c is the confining pressure. There is no difference between the deviatoric stress and an effective deviatoric stress which might take pore fluid pressure into account. The stress paths of the samples in p-q and p'-q space are given in Figure 6.9. The difference between p and p' is the pore fluid pressure.

In each case the stress behaviour is different, though D5 and D6 are most similar. The average applied stress path is typical for a drained sample (Jones, 1994, fig. 2.25). The effective stress paths, however, trend towards a critical state line (cf. Jones, 1994, fig. 2.25 and 2.28), but then move back to paths with gradients similar to those early in the tests. There is no clear yield line from which to gain Mohr-Coulomb parameters.

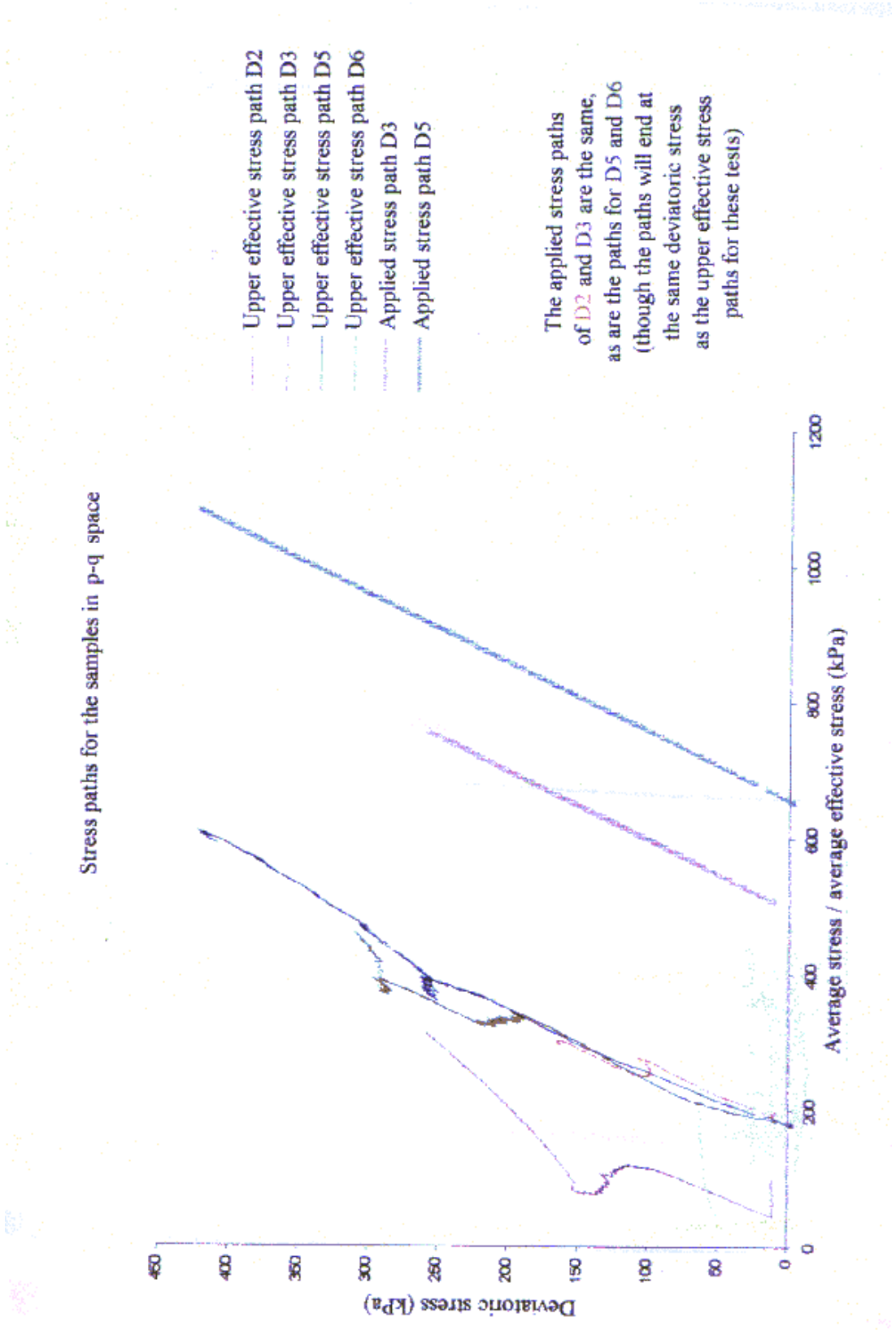

Figure 6.9 p-q space records for the triaxial tests

6.3.5 Visual scale deformation features

After deformation the samples were stiff enough to remove from the test rig without further damage. The samples were seen to have developed dislocation planes, above which the samples were shifted outwards and downwards (*Figure 6.10*). These shear planes also separated lower areas of deformation that appeared pervasive on the visual scale from upper areas that did not appear to have undergone as much destruction. Original features of sample preparation could be seen in the upper areas, whereas these were obliterated on the smoother surface of lower areas. Despite the dislocation planes and the preservation of features in the upper halves of the samples, almost all movement was by pervasive barrelling, and mostly above the shear planes.

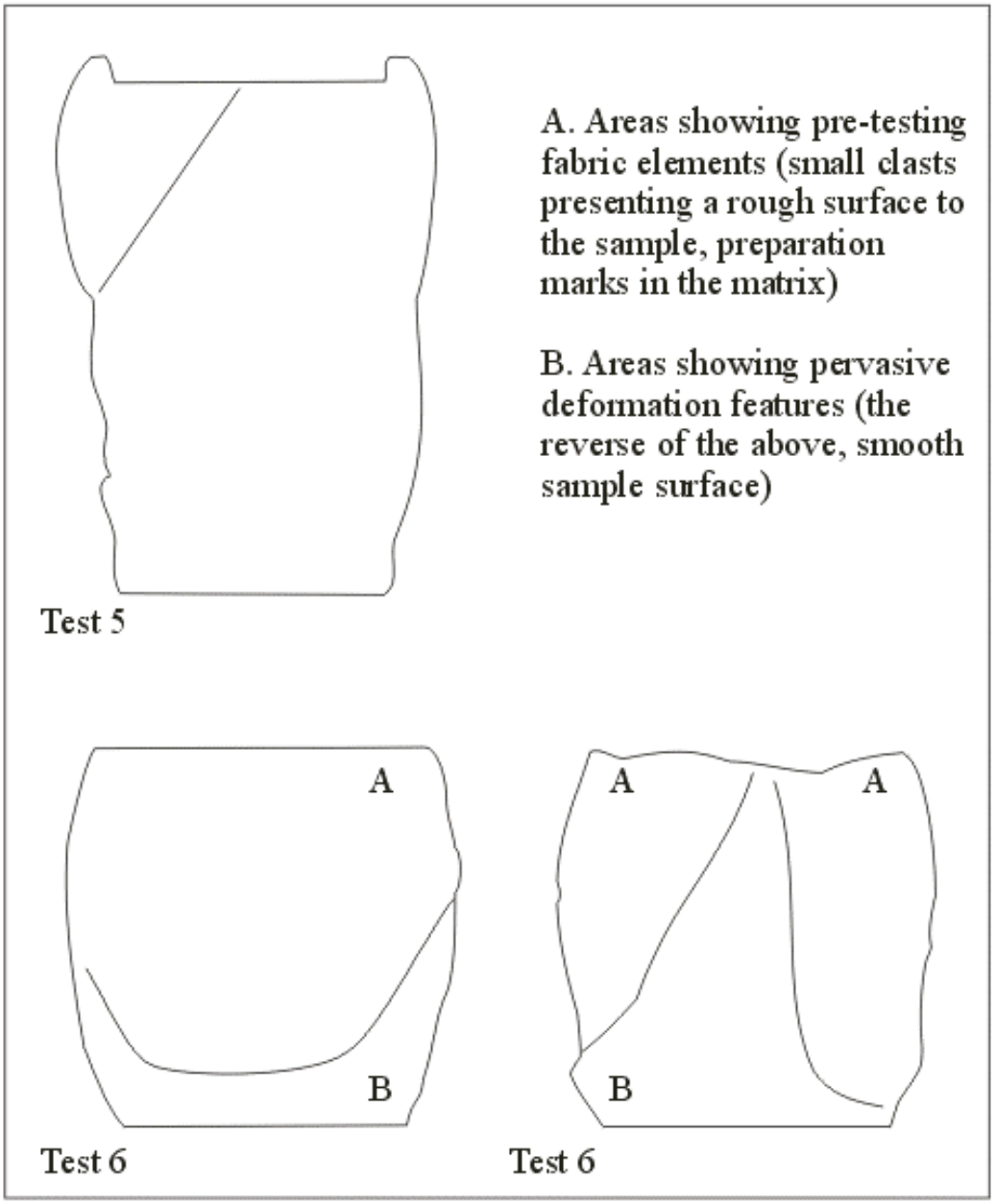

Figure 6.10 Visual scale appearance of two test samples. Test 5; cross section showing shear dip, drawn during sectioning for thin section samples. Test 6; showing outer surface after tests. Note the two dislocation planes.

6.3.6 Summary of results

The following features need explanation. They are given in their order of development.

1) Initial strain hardening of the samples coincident with a build up of pore pressure and increase in the storage of fluid (for D2 and D5) (0 to ~5%). Also, the small drops in supported stress at <2.5% strain for two samples.
2) The slowing of the fluid pressure rises without a change in the stress build-up or storage increase (between 2.5 and 7%).
3) The slowing of the stress rises, with a temporary fluctuation in stress and a simultaneous fluid *expulsion* in two samples (at ~5%).
4) The association, with this set of stress fluctuations or one prior, with a renewed increase in fluid *pressure* to a new plateau.
5) A stress fluctuation and simultaneous pore pressure increase which is followed by an equally rapid fluid pressure decline (D3 at 8%; D5 at 11.5%; D6 at 20%). There is no consistency in which stress fluctuation initiates this fluid pressure increase, though the first fluctuation always initiates either a stable (see 4, above) or unstable rise. The fluid pressure at which the rapid drop occurs is similar for similar confining pressures.
6) The work-hardening in samples (between 11 and 14%), unrelated to the fluid pressure, and its stepped profile.
7) The large variation in the responses of samples.
8) The pore fluid storage response of sample D6, which is at odds to the other reliable tests, despite showing similar responses in the other variables.

6.4 Discussion of results

This section outlines a self-consistent model of the processes based on the results above; which are often paradoxical at first sight. The events are interpreted in order of development. These interpretations are tested through comparison with the micromorphology of the test samples in Chapter Seven and related to ‘natural’ examples in Chapter Eight.

6.4.1 Initial stress and upper pore fluid pressure build up with dilation

Work by numerous authors (Chapter Three) suggests the early stress build-up in triaxial tests occurs because the sediment fabric is not optimal for strain, that is, shear zones have not yet developed. A micromorphological examination of the samples used in the triaxial tests (presented in the next chapter) indicates that they are unorientated and heterogeneous on a microscopic scale before deformation, suggesting the fabrics were not optimally arranged for stress dissipation. It should be remembered that there was no outcrop scale evidence for prior strain at the sampling location such as horizons of dilation or shear. Strain resistance due to this lack of uniform structure *may* be enhanced in the cases reported here by the increase in pore size indicated by the net storage in the samples. This dilation may result from the rising pore-fluid pressure, which will enlarge pores. However, the storage signals of both D2 and D5 are better matched by the *stress* response later in the tests. Similarly, in D6, storage does not reflect the fluid pressure signal; reduced storage changes appear where predicted on the basis of the fluid pressure, but the rises are muted. These facts indicate that dilation caused by the inflow of fluid is overprinted by the dilation caused by the applied (differential) stress. Early in the tests it appears that the dilation could be driving the pore fluid pressures' equalisation. However, this proposition does not hold up later in the tests.

The fact that dilation is not proportional to the strain shows that a large proportion of the strain is achieved without changing the samples overall volume and is undrained. The dilation appears proportional to the *increase* in supported stress at any given time. This relationship suggests that the *proportion* of volumetric deformation (dilation and compression) is related to the stress *magnitude*.

Work in other subject areas (Chapter Three) suggests that the stress-strain relationship changes because of changes in the grain orientation of the sediment, and the rise in pore-fluid pressure. The pore fluid pressure is in equilibrium prior to sample deformation, therefore, the increase in pore fluid pressure must be due to microstructural changes, which will be considerable in this previously unorganized material.

The strength of sediments is thought to be related to their effective confining pressure (*Equations 3.1* and *6.1*). The pore-fluid pressure gradient will, therefore, create a deformation gradient across the sample. This matches the form of sample D5, which showed a more marked barrelling in the upper half of the sample (*Figure 6.10*). In this situation dilation is more likely in the upper half of the sample where the fluid pressure is highest (though it is pointed out, above, that the effect of stress appears to be greater that that of fluid pressure in the sample taken as a whole).

The rise in pore-fluid pressure suggests a *reduction* in permeability, often associated with reduced pore size (discussion in Chapter Three). This contradicts the dilation implied by the storage signal. There are four possible explanations for this contradiction. In the first two, the permeability variation is between the base and top of the sample. In the third, the permeability variation is between local dilatant shear zones and the generally compressed mass of the rest of the sample. As we only record the *difference* between compression and dilation we cannot gauge the absolute size of these areas. The fourth explanation centres on tortuosity.

1) Excess pore-fluid pressure will dissipate more easily at the freely draining sample base, allowing greater stress to be transferred to the skeleton and causing pore collapse. This will decrease the permeability nearer the sample base. Under this scenario the permeability is controlled by the minimum pore neck size on the drainage path, as storage shows the bulk porosity to be increasing.

2) Prior to stress application the fluid pressure gradient across the sample is in equilibrium with the pore size down through the material. If compression occurs evenly throughout the sample, and the permeability is related to the porosity through a linear factor >1, or by a positive power law (Chapter Three), the permeability of the small pores lower down will be decreased to a greater extent than the upper ones. This will feedback as the pore pressure rises at the top of the sample. Under this scenario, the permeability, again, must be limited by the minimum pore neck size on the drainage path.

3) The dilatant areas may be incipient shear zones separated from a generally compressed mass with reduced permeability. Such incipient shears would have to be hydrologically

inactive or only active along limited pathways. This shear hypothesis accords with later events (at 7.5% and 12.5%+) which suggest the action of fully developed shears, and the presence of visual scale shear zones. If this hypothesis is true, it seems likely that such shears propagate from the high fluid pressure regions.

4) The above interpretations follow naturally from the inference that compression is responsible for the raised pore pressure. The alternative to this model is that sample tortuosity increases while dilation occurs to give net storage (tortuosity is discussed in greater detail in Chapter Three). However, it will be shown (below) that this is unlikely.

It is likely, in reality, that compression is more active lower in the sample, but that dilatant shears propagate from high in the sample and affect the throughflow. The low strain shears seen on several of the samples after testing (*Figure 6.10*) reached their lowest point of intersection with the sleeved boundary at least a third of the way up from the base platen. In fully drained or undrained tests, shears usually pass through the whole length of the sediment. This appears to confirms that shears developed in a zone *above* a lower stronger area, possibly compressive, and that the preservation of pre-test features in the upper part of the samples after testing is not a result of strength differences. These hypotheses will be examined further in a thin section study of the tested material in Chapter Seven.

Summary: The early response of the sediment to deformation is a result of the previously unorientated and heterogeneous material undergoing the transformation to a structure optimal for stress and fluid dissipation. Storage indicates dilation (which appears to vary in proportion to stress rather than raised pore fluid pressures), but pore fluid pressure suggests compression. Four possible explanations are put forward to account for this contradiction, including compression near the base of the sample and/or storage of fluid in incipient shears higher in the sample. In these hypotheses the pore fluid pressure is controlled by compression low in the sample and/or limited dilatant paths.

6.4.2 Slowing of the stress increase, storage fluctuations, and associated pore fluid pressure rises

In all of the tests there is a minor stress drop between 6 and 8% followed by a stress rise. In D2 the storage drops and returns at this point. Work by other authors comparing

micromorphology and test responses (Chapter Three) suggests this event represents the opening of a fluid throughflow channel, probably a shear. The drop in the storage curves for D2 and D5 (for a similar event at 11.5%) suggests the fluid discharge through these features has a maximum of ~3.5 mm^3 per sample interval (~0.5 to 1.5 min see *Table 6.2*). A similar drainage event occurred in test D6 at 22% (and has a similar pore fluid pressure effect; see below). There is a stress fluctuation in test D6 at 8%, but this is synchronous with *increased* storage. Here the small stress drop, and more apparent stress rise may indicate greater dilation involved in the formation of a shear zone which subsequently collapsed. A similar stress record occurred for D3 at 7%.

As these stress events end, the upper pore fluid pressure increases in D2, D5 and D6 (in D3 it keeps rising). This change backs up the hypothesis that the events represent the formation and collapse of shears, as this process has been shown to lead to decreased permeability normal to the shear strike (see review of studies in Chapter Three).

The fact that the possible collapse of dilatant shear areas does not reduce the net storage to zero may seem to go against the hypothesis that dilation is occurring in incipient shears discussed in the last section. However, such a response is in line with studies showing that shear zones are surrounded by areas of material which have undergone pervasive reorientation that do not fail (Morgenstern and Tchalenko, 1967; Tchalenko, 1968; reviewed in Chapter Three). Thin sections from the visual scale shear areas found after the tests are examined in Chapter Seven, where the hydrological effect of potential shears is further discussed.

The potential shear collapse events outlined above allow some stress release, however, this is rapidly overprinted by work-hardening, despite the higher pore-fluid pressure (cf. Equation 6.1). Unimodal sediments usually respond to shear formation by becoming weaker (see Maltman, 1994, for a review).

Summary: A number of indicators of shear formation found by other authors (Chapter Three) were witnessed during the tests. These indicators suggest that shear zones open and release some of the supported stress. There are examples of both high and low levels of prior dilation.

These shears may then have collapsed, explaining expelled fluid and the decreased permeability of the samples.

6.4.3 Catastrophic pore fluid pressure releases, and work hardening

None of the samples reach a stable supported stress, instead each work-hardens. Stress increases from ~12.5% at much the same rate as during the pervasive pre-yield movement (~<7%). The start of the hardening is not synchronous with changes in fluid pressure, infact work-hardening in D6 begins during *rising* fluid pressure in contradiction to Equation 6.1. However, hardening does *accelerate* at the same time as fluid pressure drops in three samples (D3 at 14%; D5 at 11.5%; and as fluid pressure equalises for D6 at 14%). This indicates that while pore-fluid pressure cannot initiate hardening, a drainage caused component of the hardening cannot be ruled out.

Work hardening of sediment can be attributed to areas of either dilation or compression, dependent on the packing of the sediment. These areas can be in the form of shears, for it is not necessary that shears move to release stress once they form. Shear interference by clasts may explain the lack of stress release during the main drainage events of the tests. The mass of small shears active in the pervasive deformation of fine-grained sediments (Maltman, 1987) would probably not develop strain in this sediment as they would inevitably end abutting sand grains and larger clasts (see description of sample preparation and *Table 6.1*). Movement of the material would thus have to be by the compression of the sediment matrix between clasts, and the redevelopment of any shears at inefficient orientations. These shears, again, would quickly lock as they propagated. This hypothesis of locked shears is backed up by the low strain (throws of ~2 mm) across shears seen in the samples after the tests (*Figure 6.10*). The samples strained mainly by 'pervasive' barrelling. This indicates that continuous shears could form, but were limited in their movement.

The tests show some similarities with tests on bonded rocks that have been pervasively pre-fractured (cf. Jones, 1994, p.59). However, the clarity of the material when thin sectioned (Chapter Seven), and the evidence for pervasive movement, dictates against concretion (for further information on thin sections, see Chapter Seven). The stress supported by the

sediments is higher than that usually associated with subglacial sediments tested without clasts (50-100 kPa). However, there is a small shear event early in the stress/storage records of tests D2, D3 and D6 (between 1.5% and 2.5%, also fluid discharge in D5 which may be associated with shear development) which matches the traditional yield strength of such material.

The cause of the stress plateaux in samples D5 and D6 is not understood. Alternation between work hardening and softening is a feature of cataclastic fault gouges, similar materials to tills. However, the process is not understood in this environment either (Chapter Three). As such 'stick-slip' behaviour is not found in unimodal clay or silt tested under low confining pressures, it seems likely that it is due to clast interactions with other clasts or shear zones. This hypothesis is in line with the suggestion of Simamoto and Logan (1981) that such behaviour only develops in cataclastites when the confining pressure is high enough to convert areas of the material into rock, and with the suggestion of Nasuno *et al*. (1997) that stick-slip at a higher strain frequency is due to the formation and collapse of grain-grain bridges which interrupt shear development.

The final fall in pore fluid pressure in each sample (at 14% strain for D3, 11.5% for D5, and 22% for D6), and the synchronous drop in storage for all these samples (though D3 is unreliable) suggests a drainage pathway opening. Equation 3.2 suggests that the instantaneous hydraulic conductivity of the sediments changed from 4.90×10^{-12} to 1.02×10^{-11} m s^{-1} as the drainage paths opened. *Short term* stress fluctuations during these events in tests D5 and D6 suggest some shear movement. However, the hardening after this point dictates that any movement is limited. This lack of movement dictates against the drainage being along moving shear zones, instead implying two possibilities:

1) That the fluid leaked between the sample and rubber sleeve. However, the fluid discharge through the features was similar to that potentially associated with shears above, and the fluid pressure falls were not instantaneous (D5 took a day to equilibrate to a lower fluid pressure level). The final fluid pressure was also less than that at which drainage started. These facts indicate a threshold at which channels opened and then slowly closed. An elastic response, with similar opening and closure periods would be expected for a rubber

sleeve around a perfectly smooth sample, though it is possible that the translocation of particles during drainage opened channels down the sample side.

2) That dilatant channels opened and the fluid pressure adjusted to the presence of these over time. Such dilation need not have swamped the net expulsion seen in the records. In hard rock mechanics, the opening of joints without a coincident stress release is associated with hydraulic fracturing. The fact that drainage is initiated in tests D3 and D6 at the same fluid pressure suggests hydraulic fracturing. However, the minimum effective principle stress never moves into the tensile regime during these tests (*Figure 6.9*). This means hydraulic fracturing is not occurring, unless there are small-scale tensile areas in the heterogeneous stress field of the clast-rich sediment. Instead it is likely the deviatoric stress is causing the dilation of 'shear' zones. The lack of movement indicated by the low stress release suggests particle rotation and collapse do not occur in such zones.

The stress paths for the tests (*Figure 6.9*) indicate that the thresholds mentioned above are not associated with pre-consolidation. Given that the hydraulic channels are dilatant shears, they may be those which were suggested to have collapsed earlier in the tests. This would match the above interpretation that the collapsed shears provide a barrier producing the initial raised fluid pressure. Unfortunately this hypothesis cannot be confirmed from the data.

The storage in D5 recovers from the drainage event between 15 and 20%. The record for this test suggests that an initial ~1.5 mm^3 $interval^{-1}$ change in storage brings about a 75 kPa change in pore fluid pressure before closure. This pore pressure change is not replicated in D2 at 7.5% suggesting that the fluid discharged from D2 moved through the sediment behind a dilation front, the fabric collapsing afterwards. This would cause discontinuous drainage during the event, and the effect of the drainage on the permeability would be overprinted by the permeability decrease due to the fabric collapse.

The material, thus, follows a collapse → decreased permeability → fracture → drainage cycle identical to that seen in clays by Brown and Moore (1993), and similar to the sequence suggested for the cyclic drainage of the Nankai accretionary prism (Moore, 1989; Bryne *et al.*, 1993; Maltman *et al.*, 1993b; Chapter Three). However, the range of responses from this material is far wider than those from their unimodal or mixed silt/clay sediments. This suggests

the behaviour of the material is strongly affected by the quantity and size of the clasts in it. Clasts larger than 10% of a sample width are considered to significantly alter the stress field in triaxial tests (Vickers, 1983). No clasts of this size were found in samples after testing. Thus, it is the clasts, their concentration in the sediment by collision, and their relationship with microstructures that probably give the material its wide range of responses. It is, perhaps, surprising that there is not a *wider* range of responses. The above formulation of a general response which tests vary around, provides hope that continued tests, particularly on till analogues, can further elucidate the rheology of subglacial sediments.

Summary: Work-hardening occurs, probably because clasts render any shear zones, (found in most deformed sediments), immobile. However, shear opens hydraulically active channels. These open channels are maintained, possibly because the immobility of the shears prevents collapse, or possibly because stress heterogeneities allow some hydraulic fracture. Proposed earlier shears must have propagated with collapse occurring shortly after dilation. The processes producing stick-slip behaviour of the material undergoing work-hardening may match those producing the effect in cataclastic shear zones.

6.4.4 Summary of discussion

Thus, it can be seen that the following situations develop as the material is strained:

1) The material must have initially responded with a mix of compression and dilation to give a rise in pore fluid pressure at the same time as a rise in fluid storage. Theoretical considerations suggest compression will be greater towards the sample base, while work in other fields suggests incipient shears develop early in deformation, and these might be the fluid storage areas.
2) The material undergoes a fluid expulsion associated with a minor release of supported stress. Comparison with other studies suggests that this is due to shears propagating through the material by dilation, followed almost immediately by collapse. This hypothesis is further confirmed by the fact that the pore fluid pressure rises after these events, that the variations of these events between samples can all be explained by the shear model, and by the presence of shears on a visual scale after the test. Continued dilation has little affect on the fluid pressure.

3) The pore fluid pressure of the sediment rises each time the events described in (2) occur. The work-hardening continues. As this is not seen in fine-grained sediments, the most likely reason for the work-hardening is the particle size distribution. It is possible that the movement of clasts into the shear fabrics, usually responsible for weakening sediments, causes hardening.
4) The upper pore fluid pressure eventually reaches a threshold value at which drainage channels are forced open. These open pathways are maintained. It seems likely these open pathways are either shears immobilised by clasts, or hydrofracture areas caused by tensile areas within the heterogeneous material. The drainage is only coupled to the stress response in so far as a number of stress relieving events described in (2) appear to raise the fluid pressure. The two are not coupled in any predictable way as the permeability effect of each event (2) is not certain.

There are a number of hypotheses based on the results which can be examined by looking at the microscopic evolution of the sediment as strain continues:

1) Yield events involve the (limited) development of shear zones.
2) Shears are destroyed by the multi-modal nature of the till, leading to work-hardening and a spreading of the shear strain in broad zones and/or various directions.
3) Through-flow channels are present in the sample, possibly in the form of hydraulic fractures or inactive shears.

Chapter Seven presents evidence for or against such situations from the test samples themselves, and then unaltered examples from the Skipsea Till showing the 'natural' response of the sediments are examined in Chapter Eight.

6.5 Conclusions and implications for glacial deformation

Glacial sediments respond to deformation in a number of ways. Multi-modal tills under pure shear respond by work-hardening. This opposes the work-softening seen by Kamb (1991) in *size-truncated* multi-modal sediments under simple shear with a forced shear zone. This finite-strain hardening may be representative of the initial deformation of sediment, but cannot be maintained to a steady state given the deforming beds seen by various workers (Boulton and Hindmarsh, 1987; Blake 1992). Therefore, it is supposed that the till will eventually expel

clasts from some areas allowing shear like that envisaged by Kamb to occur locally. This may have been the reason for the horizontal weakness experienced during the preparation of the sediment (above).

In Kamb's (1991) view there is no possibility of deforming beds maintaining any stress, however, there is another interpretation of his results. It is implicit in his constant strain tests that the stress representing the boundary between the two deformational behaviours *can* be supported and cause strain at the finite rates found for ice streams. This fact justifies the use of the term 'residual strength' for this value, rather than 'yield strength' as used by Kamb. Basal stress may drop down to this value under ice masses (1.5 kPa) (cf. Boulton and Jones, 1979). The potential strain rates are much lower than those predicated using $n \approx 100$ in Equation 6.1.

Such a shear stress may seem low compared with modern glaciers (~ 50 to 100 kPa), however, it may not have been such for the Dimlington ($\delta^{18}O$ Stage 2) ice sheets over Britain. The ice lobe that moved down the East coast depositing the Skipsea Till is considered to have been thin, as it originated from the relatively low altitude Cheviot Hills some 250 km to the North (*Figure 6.3*). If the 'drift' limit of Kendall (1902) is taken to represent the surface slope of the ice mass as recorded against the North York Moors (assumed flat based at sea level), the basal shear stress can be calculated as varying between 8.96 kPa at Robin Hood's Bay to 5.12 kPa at Scarborough (*Figure 6.5*). This surface slope would give a surface altitude of 1203 m over The Cheviots. The presence of ice in this area is well constrained by radiocarbon dates. Arctic mosses in silts under the tills at Dimlington (*Figure 6.5*) have been dated to a minimum of 18.01 ka B.P. (Rose, 1985) and postglacial organics in the Lake District (*Figure 6.3*) date the end of production of erratics found in the East Coast tills to ~14.3 ka B.P. However, even if the snout of the ice is considered to have left the Cheviots at 18.01 ka B.P. and 50% of the remaining period is allowed for ice degeneration, the needed advance rate is only 134.77 m a^{-1} (for a more realistic 10% deglaciation this becomes 74.87 m a^{-1}). This movement is well within the range of shear rates which produced Kamb's finite residual strength (32 m a^{-1} to 1903.2 m a^{-1}) and it is unnecessary to introduce perfect plasticity in the sediment to explain it. Thus the deformational structures produced in the East Coast tills can still be hypothesised to be of a non-meltout, deformational origin. In Chapter Eight it will be

shown that ice movement due to bed deformation in this area was supplemented by decoupling between the ice and its bed.

However, as most present ice masses *are* calculated to have basal shear stresses above Kamb's threshold figure it is necessary to look more closely at the results presented above. Two processes may lead to a stiffer sediment than that maintained by Kamb:

1) Work hardening will occur. The residual state of till will probably be a mix of areas experiencing work hardening, and those with a Kamb rheology. Work-hardening will lead to increased 'Weertman (1957) sliding' at the till surface with increased regelation melt deposition against lodging boulders (Chapter Five), giving 'constructive deposition' (Hart *et al.*, 1990). This hypothesis is testable in that the sediment's strain should vary with clast density. It should be reiterated that the work of Rutter *et al*. (1986) (see Chapter Three) shows that tails of material strung out from clasts by strain are due to clasts interfering with shears, and that it is implicit in their findings that the clasts support some of the stress the material is subjected to. The shear strength of strung-out sandstone and chalk clasts found in tills is considerably larger than that of clays and silts at subglacial effective pressures, so clast fracturing cannot be envisaged unless the clays and silts undergo work-hardening, probably because the clasts obstruct shear areas in the sediment.

2) Stress is uncoupled from the hydraulic response. The material can drain with no stress release. This leads to a stiffer sediment, without the concomitant weakness one would expect if the drainage paths were moving shear zones. The maximum discharge through such features during the tests was only 1.4897×10^{-6} m^3 day^{-1}. However, this was 52% of the potential discharge (the fluid input during this period). The instantaneous hydraulic conductivity (Chapter Three) of the sediment changed from 4.90×10^{-12} to 1.02×10^{-11} $m\,s^{-1}$ as the drainage paths opened. In traditional rock mechanics hydraulic fracture occurs perpendicular to the minimum principle stress. In these samples this direction will have been complicated by the heterogeneous stress field and/or the shear component necessary for fracture. However, subglacial hydrofracture will probably be in the direction of maximum applied stress under a pure shear geometry, and the shear stress elsewhere, ie. approximately horizontally. This will facilitate flow to the front of the glacier. Such a process

is likely to increase fluid flow in the direction of the resultant hydraulic gradients produced by the glacier profile and the fluid pressure in major channels.

It has been shown that events reduce the permeability of the sediment in the direction of the maximum applied stress. In the glacial case of stress between clasts, this would be horizontal. The permeability need not be reduced in the direction of the *minimum* applied stress (vertical glacially), provided the changes are due to tortuosity variations (Arch, 1988; Chapter Three) rather than pore size variations. If the permeability variation results from pore size changes the variation will be locally isotropic. The wider effect of the repacking will depend on the shear area facing the direction of fluid flow.

Thus, fluid pressure build-up will be accelerated subglacially. Such a rise will, however, be buffered by the channelling described above. This will lead to a dryer and stronger sediment than might be expected. It can therefore be seen that fabric collapse and dilation in subglacial sediments appears to drive their fluid pressure towards a buffered midpoint. In these tests this gave an effective confining pressure of ~200 kPa.

This chapter has examined the hydraulic and stress response of natural multi-modal glacial sediments under conditions representative of subglacial environments. The material follows a collapse → decreased permeability → fracture → drainage cycle identical to that suggested to occur in oceanic accretionary prisms. In the next chapter the interpretation of the test results are examined by looking at the micromorphology of the test samples. These results are then used to determine the stress and hydrological history of the glacier depositing the Skipsea Till and other sediments in Chapter Eight.